ELSEVIER

Journal of Alloys and Compounds 408–412 (2006) 598–602

Journal of ALLOYS AND COMPOUNDS

www.elsevier.com/locate/jallcom

# Orthorhombic distortion in $Ca_{2-x}Gd_xMnO_4$

Junichi Takahashi [a,*], Hidenori Nakada [b], Hirohisa Satoh [b], Naoki Kamegashira [b]

[a] *Institute of Multidisciplinary Research for Advanced Materials, Tohoku University, Sendai 980-8577, Japan*
[b] *Department of Materials Science, Toyohashi University of Technology, Tempaku-cho, Toyohashi 441-8580, Japan*

Received 30 July 2004; received in revised form 22 November 2004; accepted 15 December 2004
Available online 29 June 2005

**Abstract**

The crystal structure of the polycrystalline $Ca_{2-x}Gd_xMnO_4$ has been investigated by Rietveld method using X-ray diffraction patterns measured at room temperature. Within the limited substitution range, $0 < x < 0.45$, $Ca_{2-x}Gd_xMnO_4$ has the $K_2NiF_4$-type structure. In $x = 0.2$ X-ray spectrum shows the tetragonal primitive structure (space group *I*4/*mmm*). In the range of $x$ from 0.35 to 0.45 an orthorhombic superstructure (space group *Pccn*), whose unit cell relates to the tetragonal primitive structure with $a_o \approx b_o \approx \sqrt{2}a_t$, $c_o \approx c_t$, is refined. The orthorhombic superstructure contains the oxygen connected $MnO_6$ octahedra with a different tilt angle between $x$- and $y$-axes of the orthorhombic unit cell. The magnitude of the rotation of the $MnO_6$ octahedra around $x$-axis increases with increasing the substitution of $x$ in $Ca_{2-x}Gd_xMnO_4$, and that around $y$-axis shows the maximum at $x = 0.4$.


*Keywords:* $K_2NiF_4$-type oxides; Orthorhombic structure; Calcium rare-earth manganate; Oxygen octahedron

## 1. Introduction

$Ca_{2-x}Ln_xMnO_4$ solid solutions (Ln = rare earth) were originally prepared by Daoudi and Le Flem for Ln = Pr, Nd, Sm–Gd [1], and by Chaumont et al. for Ln = Y [2]. Magnetic [3,4], electric [4,5], magnetoresistance [6] and charge ordering [7] properties of the solid solutions have been recently investigated with the analogy of the perovskite, $Ca_{1-x}Ln_xMnO_3$. Phase identification showed that the $Ca_{2-x}Ln_xMnO_4$ has the $K_2NiF_4$-type structure without an ordering of Ca and Ln ions, and that there exist a limit of substitution for Ca by Ln: $x < 0.3$ for Ln = Y, $x < 0.5$ for Ln = Pr–Gd and $x < 0.45$ for other rare-earth elements [1,2,8]. According to the structural refinement of the $Ca_{2-x}Ln_xMnO_4$ series, it has been known for the sequential structure changes at room temperature that the $Ca_2MnO_{4.00}$ ($x = 0$) has a tetragonal superstructure with the apace group of $I4_1/acd$ [9,10] and that the $Ca_{2-x}Ln_xMnO_4$ ($0.05 < x < 0.25$) has the primitive tetragonal structure (*I*4/*mmm*) [8,11].

It has been confirmed that for higher values of $x$ in $Ca_{2-x}Ln_xMnO_4$ ($0.25 < x$) the corresponding phase crystallizes in the orthorhombic superstructure which is related to the primitive tetragonal structure as $a_o \approx \sqrt{2}a_t$, $b_o \approx \sqrt{2}a_t$ and $c_o \approx c_t$, where the notations of $a$, $b$ and $c$ are the unit cell parameters, and the subscripts o and t refer to the orthorhombic and the tetragonal, respectively. The structural phase transition of the orthorhombic structure was studied by use of high- and low-temperature X-ray and electron diffractometry: The orthorhombic structure of $Ca_{1.5}Nd_{0.5}MnO_4$ changes to the primitive tetragonal one between 294 and 393 K [4] and $Ca_{1.7}Sm_{0.3}MnO_4$ undergoes a low-temperature tetragonal phase below around 70 K [8,11,12]. The orthorhombic structure of the $Ca_{2-x}Ln_xMnO_4$ was predicted to have the space group of *F*222, *Fmm*2 or *Fmmm* [1]. The electron diffraction pattern of $Ca_{1.75}Pr_{0.25}MnO_4$ showed two kinds of the candidate structure with *Cmca* (*Abma*) or *C*2*cb* as possible space groups (*Cmca* was chosen in their paper) [7]. Another kind of an orthorhombic structure with a space group of *Pccn* possesses in the $K_2NiF_4$-type oxides of $(La,Nd)_2CuO_4$ [13], $(La,Nd,Sr)_2CuO_4$ [14], $(La,Sm,Sr)_2CuO_4$ [15] and $(La,Ba)_2CuO_4$ [16] as in the low-temperature phase.

* Corresponding author. Tel.: +81 22 217 5161; fax: +81 22 217 5211.
*E-mail address:* junichi@tagen.tohoku.ac.jp (J. Takahashi).

0925-8388/$ – see front matter © 2005 Elsevier B.V. All rights reserved.
doi:10.1016/j.jallcom.2004.12.150

In this paper, the crystal structure of the orthorhombic $Ca_{2-x}Gd_xMnO_4$ with a $K_2NiF_4$-type structure was analyzed by the X-ray powder diffraction and the Rietveld analysis on the basis of the candidate structure models, *Fmmm*, *Abma* and *Pccn*.

## 2. Experimental

Polycrystalline $Ca_{2-x}Gd_xMnO_4$ series were prepared from powders of $CaCO_3$ (4N-purity), $Gd_2O_3$ (4N) and $Mn_2O_3$ (3N) by solid-state reaction. The raw powders were pre-heated before weighting and mixing by the followings. $CaCO_3$ was heated at 673 K for 24 h in $CO_2$-gas and then slowly cooled to room temperature without stopping gas flow, $Gd_2O_3$ was treated with heating at 1273 K for 24 h in Ar-gas and then slowly cooled to room temperature without stopping gas flow, $Mn_2O_3$ was annealed at 1073 K for 72 h in air and then quenched to room temperature. These powders were mixed in a required atomic ratio with an agate mortar and pressed into pellets, which were then put into platinum boat. The pellets were fired at 1523 K for 72 h in air, followed by slowly cooled to room temperature.

X-ray powder diffraction data of the sample were measured using a diffractometer system equipped with a single crystal graphite monocromator (MAC MXP$^{18}$ powder X-ray diffractometer). Diffraction patterns were collected with Cu Kα radiation over a $2\theta$ range from 20° to 109° with a step width of 0.04° and counting time of 4.5–6.0 s (variable). The structural refinement was carried out by the Rietveld method (a computer program RIETAN [17,18]) using the whole $2\theta$ ranges of the collected diffraction data.

## 3. Results and discussion

Some raw materials were detected after calcinations of the sample with $x$ values higher than 0.45 with the initial composition of $Ca_{2-x}Gd_xMnO_4$. This limitation of the element substitution is agreed with the previous report [1]. Fig. 1 shows the X-ray powder diffraction patterns of (a) $Ca_{1.8}Gd_{0.2}MnO_4$ and (b) $Ca_{1.6}Gd_{0.4}MnO_4$. It can be seen from Fig. 1a that $Ca_{1.8}Gd_{0.2}MnO_4$ has the primitive tetragonal cell (space group *I*4/*mmm*, unit cell dimension as $a_t \times a_t \times c_t$), which is so-called T structure. The X-ray diffraction pattern of $Ca_{1.6}Gd_{0.4}MnO_4$ (Fig. 1b) can be indexed with the orthorhombic superstructure, whose cell dimensions relate to $a_o \approx b_o \approx \sqrt{2}a_t$ and $c_o \approx c_t$, since the peaks corresponding to $h\,h\,l$ in the T structure are splitted into $h\,k\,l$ and $k\,h\,l$ in the orthorhombic structure. This relationship reveals that the orthorhombic superstructure is distorted along the [1 1 0] direction of the T structure.

Fig. 2 shows the selected range of the X-ray powder diffraction pattern with the Rietveld refinement results for $Ca_{1.6}Gd_{0.4}MnO_4$ on the basis of the three space groups of *Fmmm*, *Abma* and *Pccn*. The structure model with the space

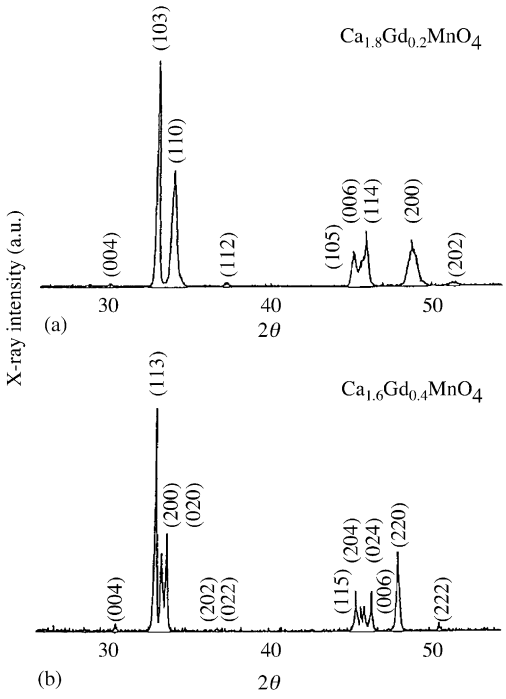


Fig. 1. X-ray powder diffraction data (Cu Kα) of (a) $Ca_{1.8}Gd_{0.2}MnO_4$ and (b) $Ca_{1.6}Gd_{0.4}MnO_4$.

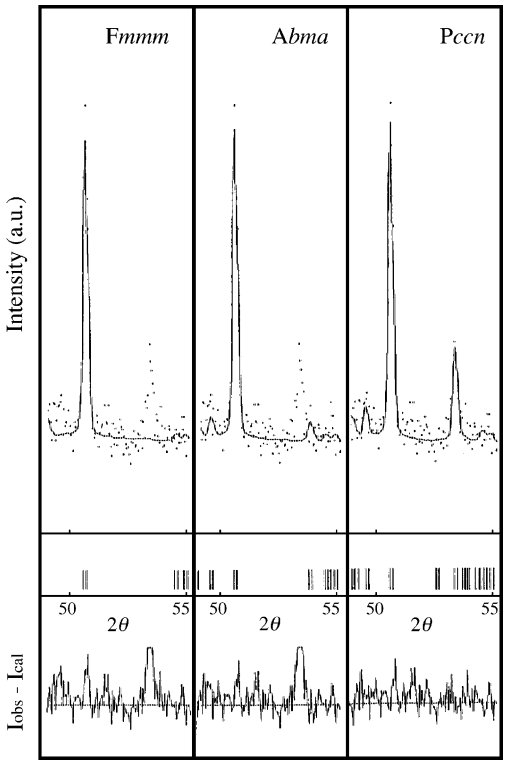


Fig. 2. The results of the Rietveld refinement for $Ca_{1.6}Gd_{0.4}MnO_4$ based on the structure models with the space groups of *Fmmm*, *Abma* and *Pccn*.

group of *Pccn* indicates that the refined profile curve is well agreed with superlattice line at $2\theta = 53.4^\circ$. In contrast, no superlattice line around $2\theta = 53^\circ$ appears in the case of the *Fmmm* and *Abma* structure models. The relative peak intensity at $2\theta = 53.4^\circ$ against the maximum one at $2\theta = 32.9^\circ$ (113 main peak, see Fig. 1b) is about 0.014, which is sensitive but measurable in the X-ray powder diffraction method. These facts suggest that the space group *Pccn* is most probable for the structure model of the distorted orthorhombic superstructure for the $Ca_{1.6}Gd_{0.4}MnO_4$.

The refined cell-constants, coordinations and *R*-factors for $Ca_{2-x}Gd_xMnO_4$ with the orthorhombic *Pccn* structure are summarized in Table 1. When we applied the *Fmmm* and *Abma* structure models to the refinement for the X-ray diffraction pattern of $Ca_{1.6}Gd_{0.4}MnO_4$, higher values of *R*-factors were resulted in, such as, for the *Fmmm* with $R_{wp} = 11.01$, $R_e = 7.26$, $R_I = 2.28$ and $R_F = 2.38\%$; for the *Abma* with $R_{wp} = 10.96$, $R_e = 7.26$, $R_I = 2.38$ and $R_F = 3.05\%$. By comparison, the *R*-factors for *Pccn* structure model showed smallest values. Therefore, it is confirmed that the space group *Pccn* is the most reliable for the distorted orthorhombic superstructure of the $Ca_{2-x}Gd_xMnO_4$.

Table 1
The refined cell parameters and *R*-factors for $Ca_{2-x}Gd_xMnO_4$

| Space group *x* in composition | *Pccn* | | |
|---|---|---|---|
| | 0.35 | 0.40 | 0.45 |
| Cell constant | | | |
| *a* (nm) | 0.5322 1) | 0.5332 (1) | 0.5340 (1) |
| *b* (nm) | 0.5361 (1) | 0.5378 (1) | 0.5382 (1) |
| c (nm) | 1.1755 (4) | 1.1735 (1) | 1.1735 (1) |
| Fractional coordinates | | | |
| Ca | | | |
| *x* | 0.00 (2) | 0.00 (3) | 0.000 (3) |
| *y* | 0.010 2) | 0.010 (2) | 0.010 (2) |
| *z* | 0.3571 (4) | 0.3573 (2) | 0.3571 (2) |
| $B_{eq}$ (nm$^2$) | 0.00 (2) | 0.004 (1) | 0.002 (1) |
| Mn | | | |
| *x* | 0 | 0 | 0 |
| *y* | 0 | 0 | 0 |
| *z* | 0 | 0 | 0 |
| $B_{eq}$ (nm$^2$) | 0.03 (2) | −0.000 (1) | 0.00045 (9) |
| O1 | | | |
| *x* | −0.00 (7) | −0.01 (1) | −0.015 (8) |
| *y* | −0.029 (9) | −0.03 (1) | −0.028 (5) |
| *z* | 0.167 (2) | 0.1654 (9) | 0.1653 (9) |
| $B_{eq}$ (nm$^2$) | 0.0023 (5) | 0.012 (4) | 0.021 (4) |
| O2 | | | |
| *x* | 0.25 | 0.25 | 0.25 |
| *y* | 0.25 | 0.25 | 0.25 |
| *z* | 0.005 (13) | 0.015 (9) | 0.013 (5) |
| $B_{eq}$ (nm$^2$) | 0.01 (3) | 0.002 (4) | 0.0 (2) |
| O3 | | | |
| *x* | 0.25 | 0.25 | 0.25 |
| *y* | 0.75 | 0.75 | 0.75 |
| *z* | −0.007 (9) | −0.009 (10) | −0.014 (7) |
| $B_{eq}$ (nm$^2$) | 0.03 (3) | 0.007 (5) | −0.00 (3) |
| $R_{wp}$ | 15.13 | 10.12 | 9.65 |
| $R_p$ | 12.06 | 7.77 | 7.16 |
| $R_e$ | 7.08 | 7.25 | 7.10 |
| $R_I$ | 3.72 | 1.89 | 2.68 |
| $R_F$ | 2.72 | 2.05 | 3.47 |
| $S = R_{wp}/R_e$ | 2.14 | 1.40 | 1.36 |

*Note:* Estimated standard deviations in the parentheses refer to the fast significant digits.

It is well known that $Mn^{3+}$ ion is the typical Jahn–Teller ion modifying $MnO_6$ octahedra, and that the orthorhombic distortion is introduced by the $Mn^{3+}/Mn^{4+}$ mixed valence state caused by the substitution of $Ca^{2+}$ by $Ln^{3+}$. Unfortunately, quantities of the anisotropic J–T distortion in the $K_2NiF_4$-type oxides is hard to assess compared to the perovskite-type one, in particular, $LaMnO_3$ [19]. For example, $MnO_6$ octahedra in pure $Ca_2MnO_4$, which consists of only non J–T ions ($Mn^{4+}$), are apparently distorted: Mn–O length is 0.185 nm within the *ab* plane and 0.192 nm along the *c* direction [10].

The $K_2NiF_4$-type structures with the space group of *Fmmm*, *Abma* (*Cmca*, *Bmab*) and *Pccn* are shown in Fig. 3. These crystal structures are distinguished with a displacement of oxygen ions concerning the $BO_6$ octahedra. In the *Fmmm* superstructure (Fig. 3a) the oxygen ions in the *ab* plane move toward [1 1 0] and [−1 1 0] directions within the plane as the position of the oxygen ions are (1/4, 1/4, 0) and (0, 0, *z*). In *Abma* model oxygen $O_2$ ions at (1/4, 1/4, *z*) move to [0 0 1]

Table 2
Interatomic distances within 3.0 Å in $Ca_{2-x}Gd_xMnO_4$

| *x* | 0.35 | 0.40 | 0.45 |
|---|---|---|---|
| Ca | | | |
| O1 | 0.224 (1) | 0.226 (1) | 0.226 (1) |
| O2 | 0.249 (1) | 0.248 (1) | 0.250 (1) |
| O3 | 0.268 (8) | 0.275 (3) | 0.277 (2) |
| O4 | 0.290 (1) | 0.293 (1) | 0.290 (1) |
| O5 | 0.268 (8) | 0.261 (3) | 0.260 (2) |
| O6 | 0.254 (3) | 0.262 (4) | 0.256 (4) |
| O7 | 0.261 (2) | 0.257 (4) | 0.256 (4) |
| O8 | 0.251 (3) | 0.245 (3) | 0.247 (2) |
| O9 | 0.245 (2) | 0.249 (4) | 0.250 (3) |
| Mn | | | |
| O1 | 0.1971 (5) | 0.1950 (5) | 0.1947 (5) |
| O2 | 0.1890 (2) | 0.1901 (4) | 0.1901 (2) |
| O3 | 0.1896 (2) | 0.1896 (4) | 0.1897 (2) |
| O2–O3a[a] | 0.2663 (3) | 0.2667 (3) | 0.2671 (2) |
| O2–O3b[a] | 0.2690 (3) | 0.2703 (3) | 0.2701 (3) |
| O1–O2 | 0.276 (5) | 0.272 (4) | 0.273 (3) |
| O1–O2 | 0.270 (5) | 0.273 (4) | 0.271 (3) |
| O1–O3a[a] | 0.269 (5) | 0.270 (4) | 0.270 (4) |
| O1–O3b[a] | 0.278 (5) | 0.274 (5) | 0.274 (4) |

[a] a, Along *a*-axis; b, along *b*-axis.

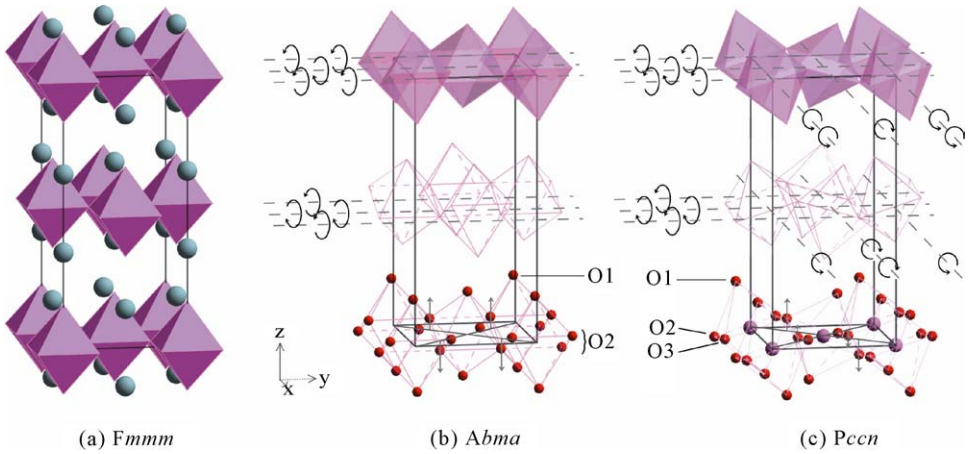


Fig. 3. Structure models of the orthorhombic $K_2NiF_4$-type oxides, $A_2BO_4$, with the space group of (a) *Fmmm*, (b) *Abma* and (c) *Pccn*. The straight and cyclic allows indicate a direction of the oxygen displacement and of the rotation of the $BO_6$ octahedra, respectively.

and [0 0 −1] directions (toward *z*-axis) as shown by straight allows in Fig. 3b. The *Pccn* superstructure is similar to the *Abma*, but the magnitude of the displacement of oxygen ions is different between O2 at (1/4, 1/4, *z*) and O3 at (1/4, 3/4, *z*′) with $z \neq z'$, as shown in Fig. 3c.

In contrast, the orthorhombic lattice distortion as a rotation of $BO_6$ octahedra can be interpreted. In the *Fmmm* structure model the $MnO_6$ octahedra have no rotation. The rotated $MnO_6$ octahedra possess in both *Abma* model and *Pccn* model; the former model involves $MnO_6$ octahedra rotated along *y*-axis of the T structure (*I*4/*mmm*) and the latter the $MnO_6$ octahedra rotated along both *x*- and *y*-axes of the T structure. As shown in Fig. 4, the rotation of the $MnO_6$ octahedra is expressed by $|\varphi_1| = |\varphi_2| = 0$ for the *Fmmm* structure, $|\varphi_1| = 0$ and $|\varphi_2| \neq 0$ for *Abma* one, and $|\varphi_1| \neq |\varphi_2| \neq 0$ for *Pccn* one, where $\varphi$ refers to the tilt angle. The calculated values of tilt angle for $Ca_{2-x}Gd_xMnO_4$ with *Pccn* superstructure resulted in $\varphi_1 = 3.01$ and $\varphi_2 = 0.51$ for $x = 0.35$, $\varphi_1 = 5.98$ and $\varphi_2 = 1.51$ for $x = 0.4$ and $\varphi_1 = 6.72$ and $\varphi_2 = 0.25$ for $x = 0.45$. The angle $\varphi_1$ increases with an increase of *x*. On the other hand, the angle $\varphi_2$ shows the maximum with $x = 0.4$. In addition, as shown in Table 1, the absolute values of the coordination *z* between O2 and O3 for $x = 0.4$ in $Ca_{2-x}Gd_xMnO_4$ are different, while those for $x = 0.35$ and 0.45 are close to each other. These trends of the change in the tilt angle $\varphi$ and the oxygen displacement toward [0 0 1] direction predict the distorted-orthorhombic superstructure-transformation as a sequence of a pseudo-*Abma* ($x = 0.35$), *Pccn* ($x = 0.4$), and the pseudo-*Abma* ($x = 0.45$) by increasing of *x* in $Ca_{2-x}Gd_xMnO_4$.

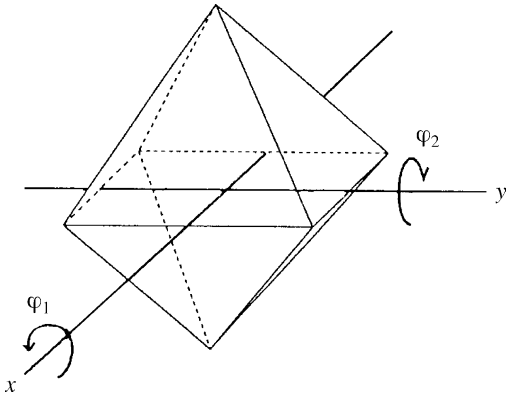


Fig. 4. Rotation of $MnO_6$ octahedra.

## 4. Conclusions

The $Ca_{2-x}Gd_xMnO_4$ solid solutions crystallized in $K_2NiF_4$-type structure with a space group of $I4_1/acd$ ($x = 0$), *I*4/*mmm* ($x = 0.2$), *Pccn* ($0.35 \leq x \leq 0.45$). The orthorhombic *Pccn* structure contained the tilted $MnO_6$ octahedra with a different angle between *x* and *y*-axes of the unit cell. The most distorted orthorhombic structure was found in $Ca_{1.6}Gd_{0.4}MnO_4$, in which the bending angle of Mn–O–Mn taken along the *ab* plane was around 170°.

## Acknowledgement

This work was supported by the Grant-in-Aid for Scientific Research by the Japan Society for the Promotion of Science.

## References

[1] A. Daoudi, G. Le Flem, J. Solid State Chem. 5 (1972) 57.
[2] C. Chaumont, A. Daoudi, G. Le Flem, P. Hagenmuller, J. Solid State Chem. 14 (1975) 335.
[3] C.R. Michel, R. Amigo, N. Casan-Pastor, Chem. Mater. 11 (1999) 195.
[4] N. Kamegashira, A. Shimono, H.W. Xu, H. Satoh, K. Hayashi, T. Kikuchi, Mater. Chem. Phys. 26 (1990) 483.
[5] W.H. Jung, E. Iguchi, J. Phys. D: Appl. Phys. 31 (1998) 794.
[6] A. Maignan, C. Martin, G. Van Tendeloo, M. Hervieu, B. Raveau, J. Mater. Chem. 8 (1998) 2411.

[7] C. Autret, R. Retoux, M. Hervieu, B. Raveau, Chem. Mater. 13 (2001) 4745.
[8] J. Takahashi, N. Kamegashira, Mater. Res. Bull. 28 (1993) 451.
[9] M.E. Leonowicz, K.R. Poeppelmeier, J.M. Longo, J. Solid State Chem. 59 (1985) 71.
[10] J. Takahashi, N. Kamegashira, Mater. Res. Bull. 28 (1993) 565.
[11] J. Takahashi, T. Kikuchi, H. Satoh, N. Kamegashira, J. Alloys Compds. 192 (1993) 96.
[12] H. Saito, Y. Inoue, F. Munakata, M. Yamanaka, J. Takahashi, N. Kamegashira, Y. Koyama, Physica C 235–240 (1994) 753.
[13] M.K. Crawfold, R.L. Harlow, E.M. McCarron, W.E. Farneth, N. Herron, H. Chou, D.E. Cox, Phys. Rev. B47 (1993) 11623.
[14] M.K. Crawfold, R.L. Harlow, E.M. McCarron, W.E. Farneth, J.D. Axe, H. Chou, Q. Huang, Phys. Rev. B44 (1991) 7749.
[15] Y. Koyama, Y. Wakabayashi, S.-I. Nakamura, Y. Inoue, K. Shinohara, Phys. Rev. B48 (1993) 9710.
[16] N. Hara, T. Kamiyama, I. Kamata, I. Nakahara, H. Hayakawa, E. Akiba, H. Asano, Solid State Comm. 82 (1992) 975.
[17] F. Izumi, J. Crystallogr. Soc. Jpn. 27 (1985) 23 (in Japanese).
[18] F. Izumi, J. Mineral. Soc. Jpn. 17 (1985) 37 (in Japanese).
[19] J. Rodrigues-Carvajal, M. Hennion, F. Moussa, A.H. Moudden, L. Pinsard, A. Revcolevschi, Phys. Rev. 57 (1998) R3189.